Supporting Information

Tuning interfacial *H coverage and aldehyde adsorption configuration for selective electrocatalytic hydrogenation of furfural

Min Zheng, Pengtang Wang, Yingjie Gao, Chen Peng, Yao Zheng*, Shi-Zhang Qiao*

School of Chemical Engineering, The University of Adelaide, Adelaide, SA 5005, Australia

*Corresponding authors

Email addresses: yao.zheng01@adelaide.edu.au (Y. Zheng), s.qiao@adelaide.edu.au (S.-Z. Qiao)

Supplementary procedures

Chemicals

Palladium (II) acetylacetonate ($Pd(acac)_2$), copper (II) chloride ($CuCl_2$), iron (III) chloride hexahydrate ($FeCl_3 \cdot 6H_2O$), oleylamine ($C_{18}H_{35}NH_2$), acetone (C_3H_6O), ethanol (C_2H_6O), cyclohexane (C_6H_{12}), and ascorbic acid ($C_6H_8O_6$) were purchased from Sigma-Aldrich without further purification. Commercial Pd/C (20 wt%), carbon paper and Nafion 117 membrane (Dupont) were purchased from The Fuel Cell Store, USA. Milli-Q ultrapure water (18.2 MΩ·cm) was used in all experiments.

In situ surface-enhanced Raman spectroscopy (SERS)

In situ SERS was conducted on a Renishaw inVia Qontor confocal Raman spectrometer with a 532 nm solid laser as the excitation source. The measurements were carried out on a screen-printed microelectrode (Pine Research RRPE1002C) with three-electrode configuration. The working electrode was fabricated by drop-casting catalysts onto the screen-printed electrode. A carbon electrode and an Ag/AgCl were used as the counter electrode and the reference electrode, respectively. The Raman spectrum of each scan was accumulated by 2 acquisitions (20 s per acquisition)

In situ attenuated total reflectance Fourier transform infrared spectroscopy (ATR-FTIR)

ATR-FTIR was performed on a Thermo-Fisher Nicolet iS50R spectrometer equipped with a liquid nitrogen-cooled HgCdTe (MCT) detector and a VeeMax III ATR accessory (Pike Technologies). A germanium prism coated with catalysts by air-brushing was used as the working electrode and was mounted in a custom-made three-electrode electrochemical cell. A saturated Ag/AgCl and a Pt wire were used as the reference electrode and the counter electrode, respectively. For each spectrum, the data were acquired by averaging 64 scans collected at a spectral resolution of 4 cm^{-1}. For furfural hydrogenation, the electrolyte used was H_2SO_4 solution with different pH values containing 20 mM furfural and was constantly purged with Ar during the experiment. The chronoamperometric tests were conducted from the potential range of 0 to −0.4 V vs RHE. The spectra recorded under open circuit potential were used as background measurements. The spectra were processed in the OMNIC software.

Supplementary Figures and Tables

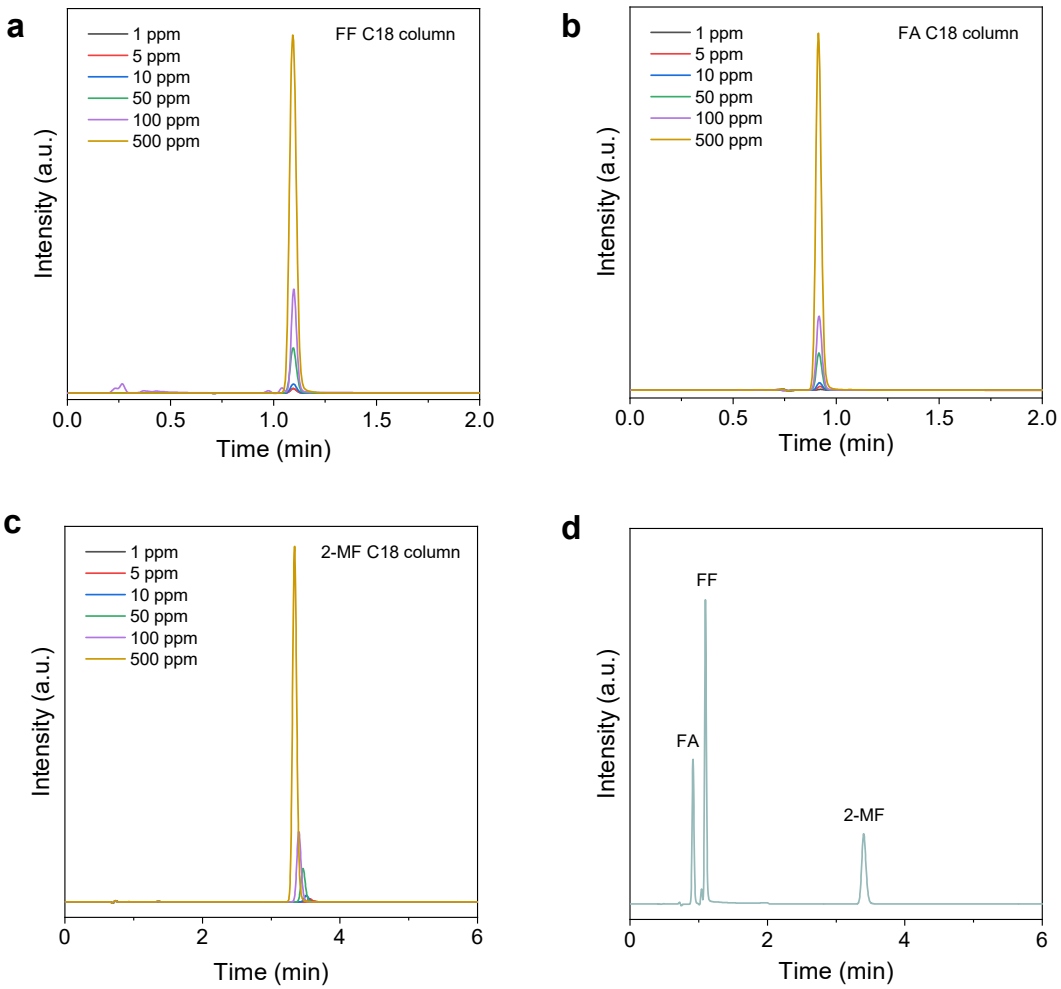

Figure S1. The standard calibration curves of (a) FF, (b) FA, and (c) 2-MF. (d) HPLC curve of all liquid chemicals.

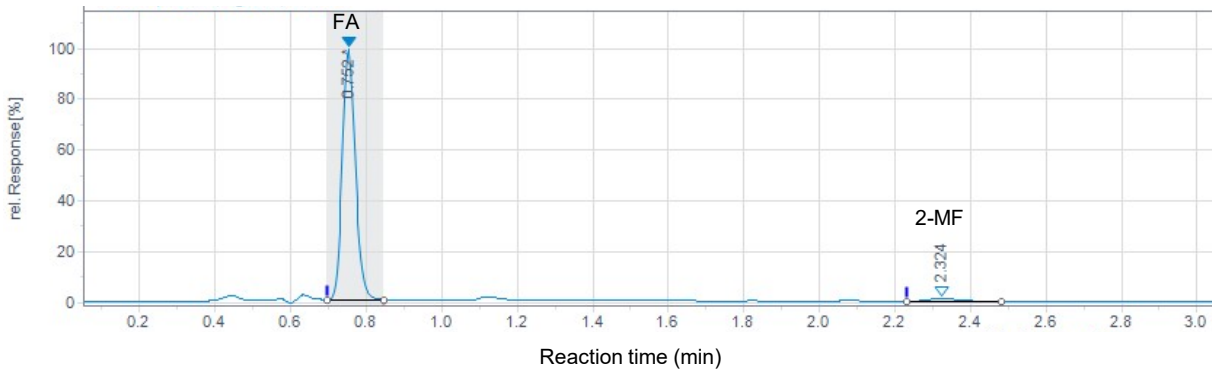

Figure S2. Electrocatalytic reduction of FA to 2-MF with a conversion efficiency of 2.1%.

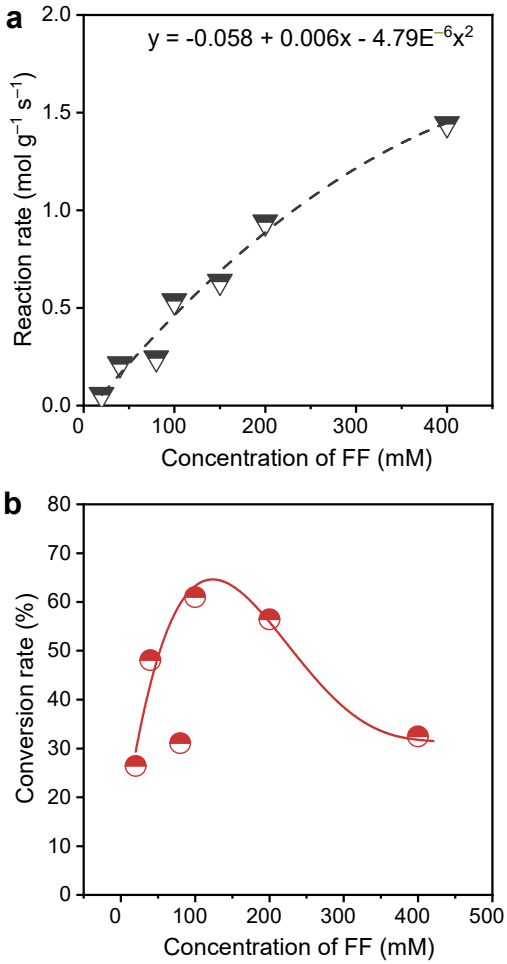

Figure S3. (a) Reaction rate, (b) conversion rate, and corresponding fitting results of FF ECH.

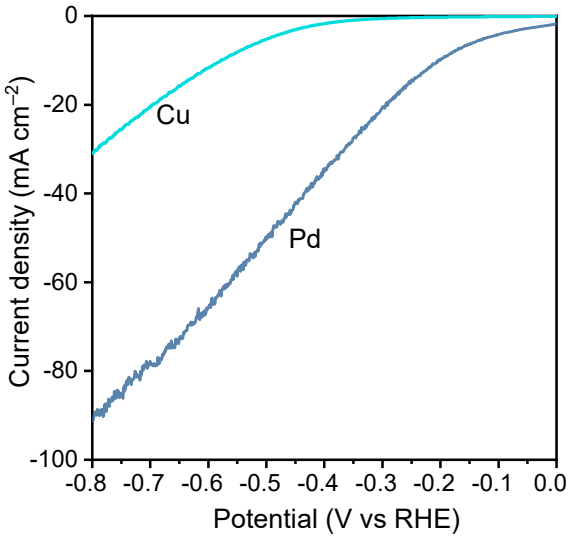

Figure S4. Linear sweep voltammetry curves of Cu and Pd for FF ECH.

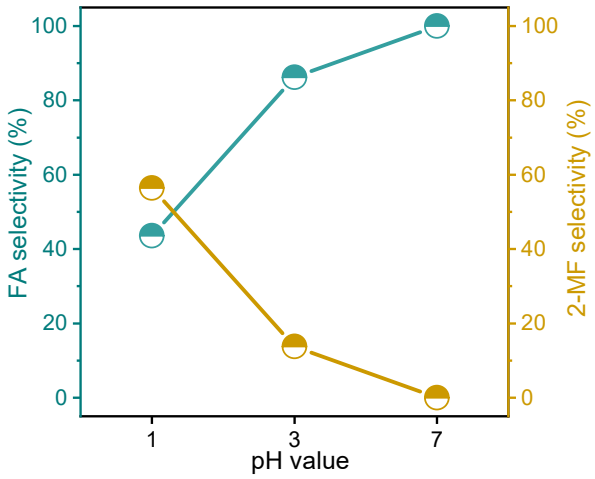

Figure S5. Selectivity of FA and 2-MF production in different pH solutions.

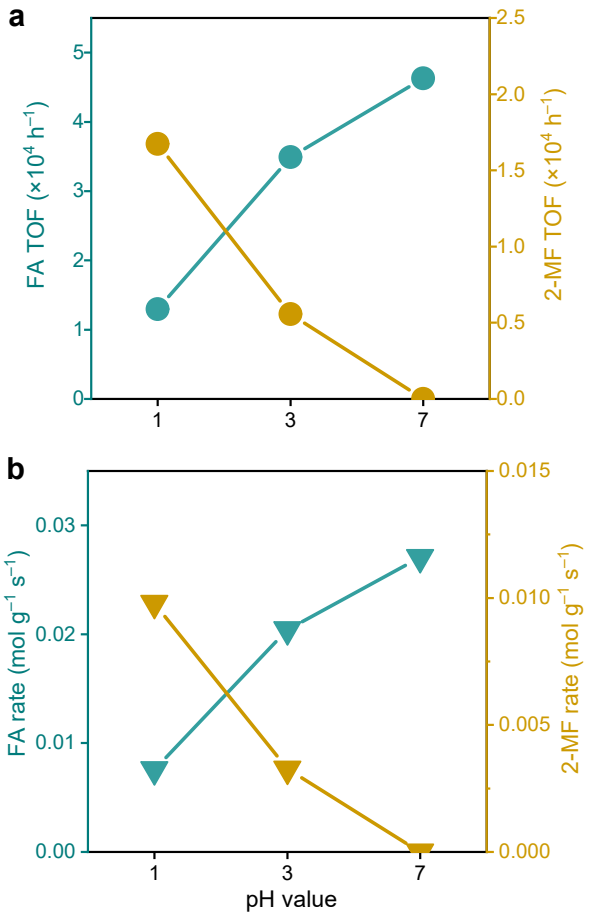

Figure S6. (a) TOF of FA and 2-MF, (b) the production rate of FA and 2-MF in solutions with different pH.

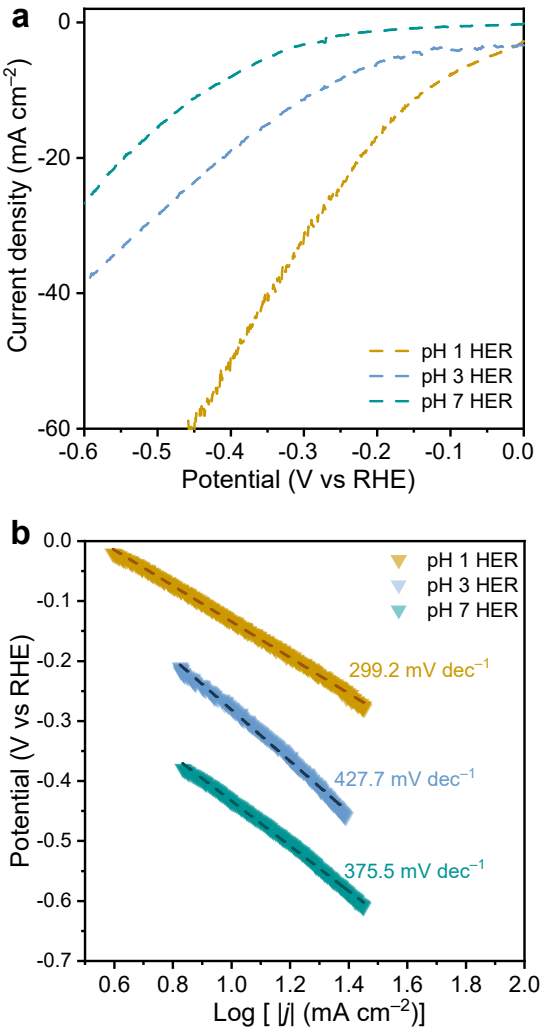

Figure S7. (a) The LSV curves for HER. (b) Tafel plots for HER in different pH solutions.

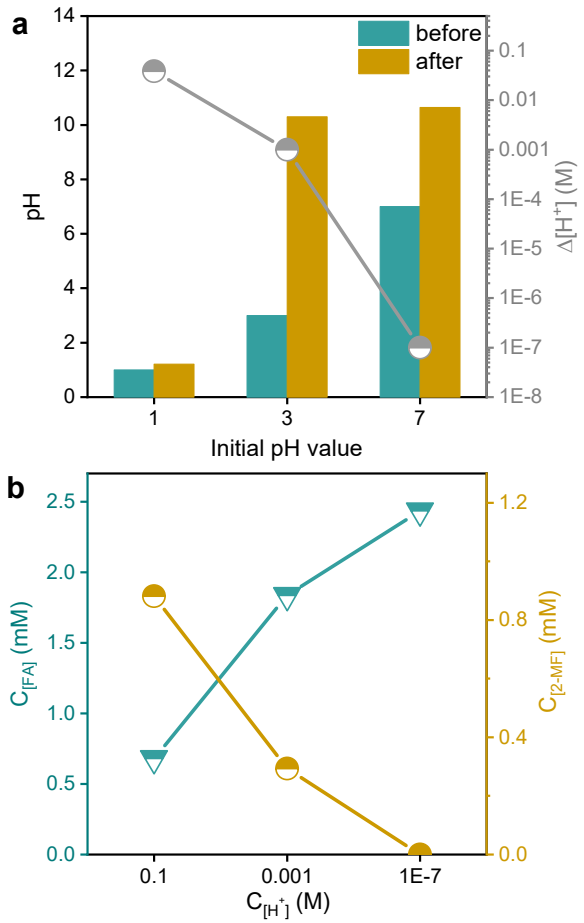

Figure S8. (a) Detection of pH values before and after reaction and consumption of H^+ concentration for different pH solutions. (b) The change in FA and 2-MF concentration as a function of H^+ concentration.

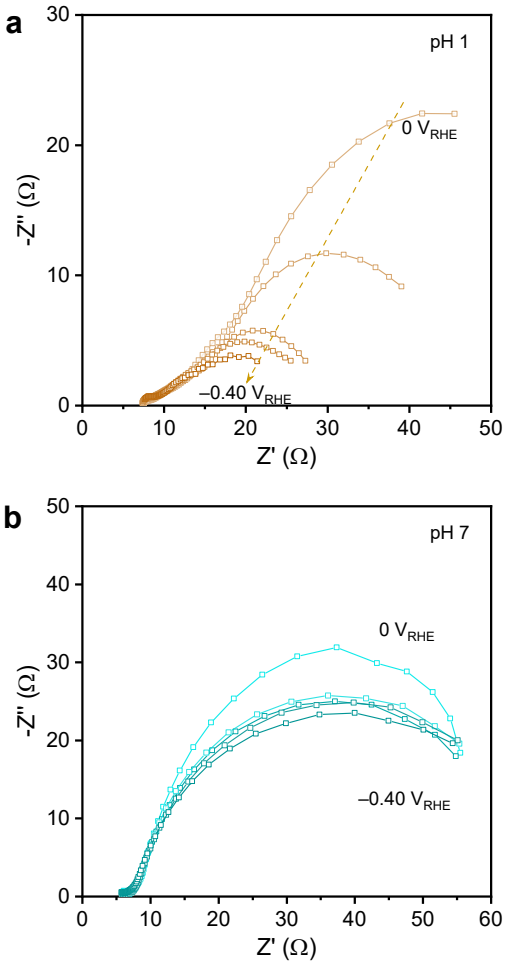

Figure S9. (a) EIS Nyquist circles under different potentials for pH 1. (b) EIS Nyquist circles under different potentials for pH 7.

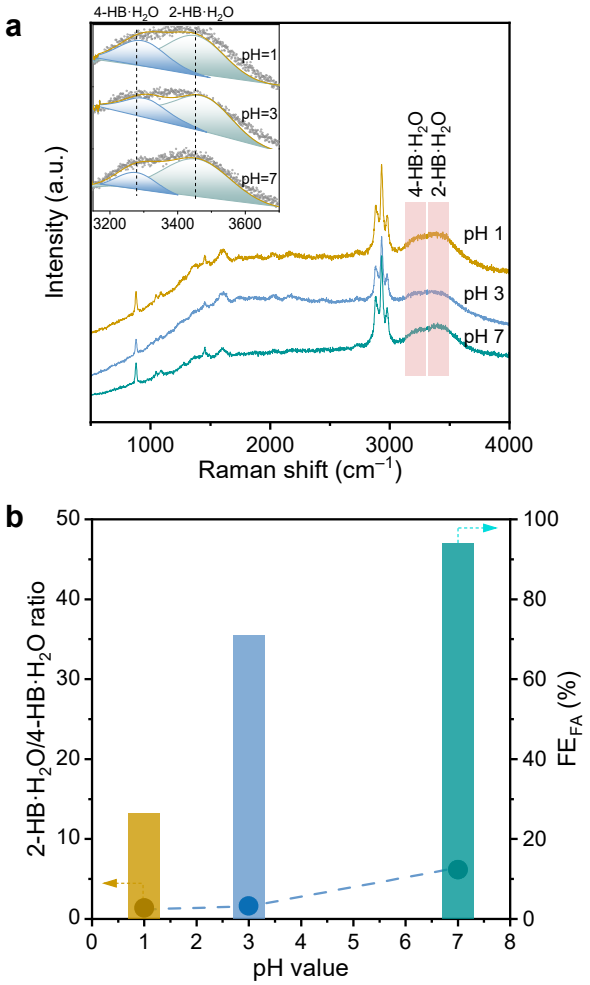

Figure S10. (a) SERS spectra for Pd/C catalyst in different pH (Inset: fitting of water peaks). (b) Calculated 2-HB·H_2O/4-HB·H_2O ratio and FE of FA as a function of pH.

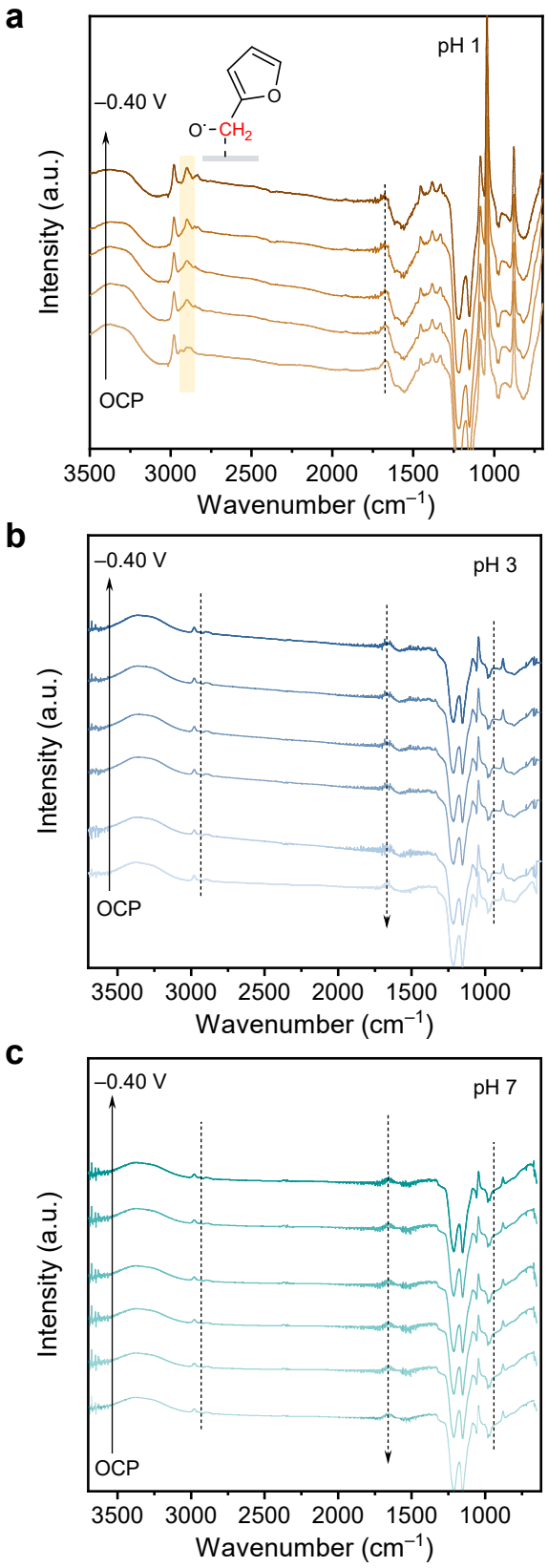

Figure S11. In situ ATR-FTIR spectra for furfural electrohydrogenation in H_2SO_4/Na_2SO_4 mixed solution with (a) pH 1, (b) pH 3, and (c) pH 7.

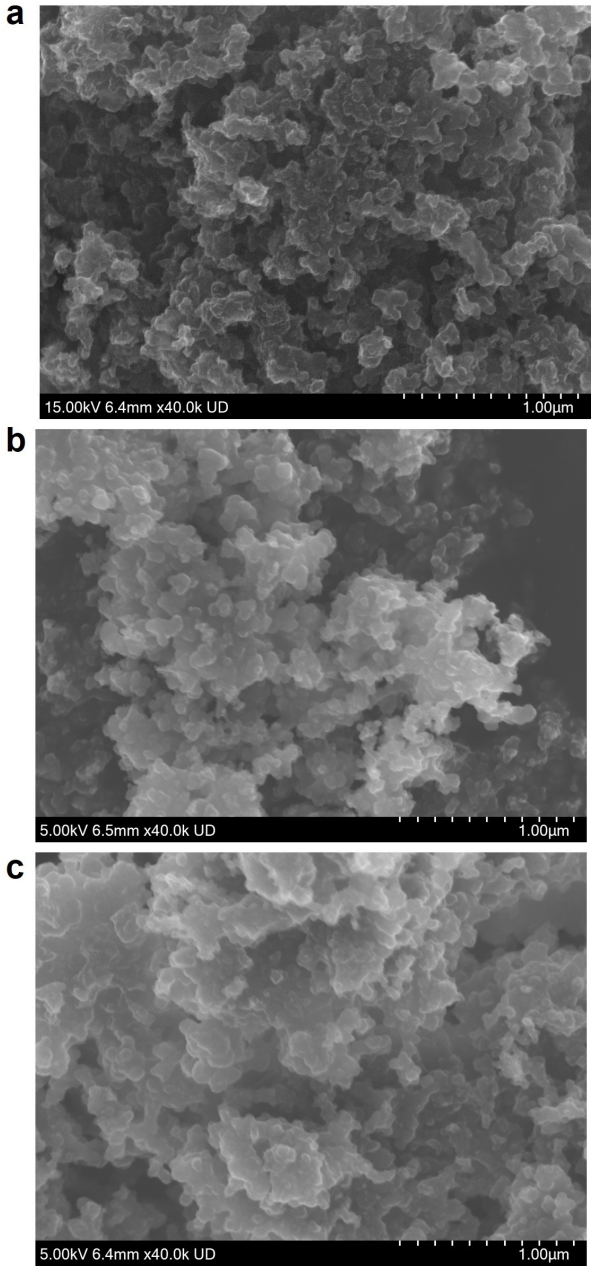

Figure S12. SEM images of (a) $PdCu_{0.5}$, (b) $PdCu_1$, and (c) $PdCu_2$.

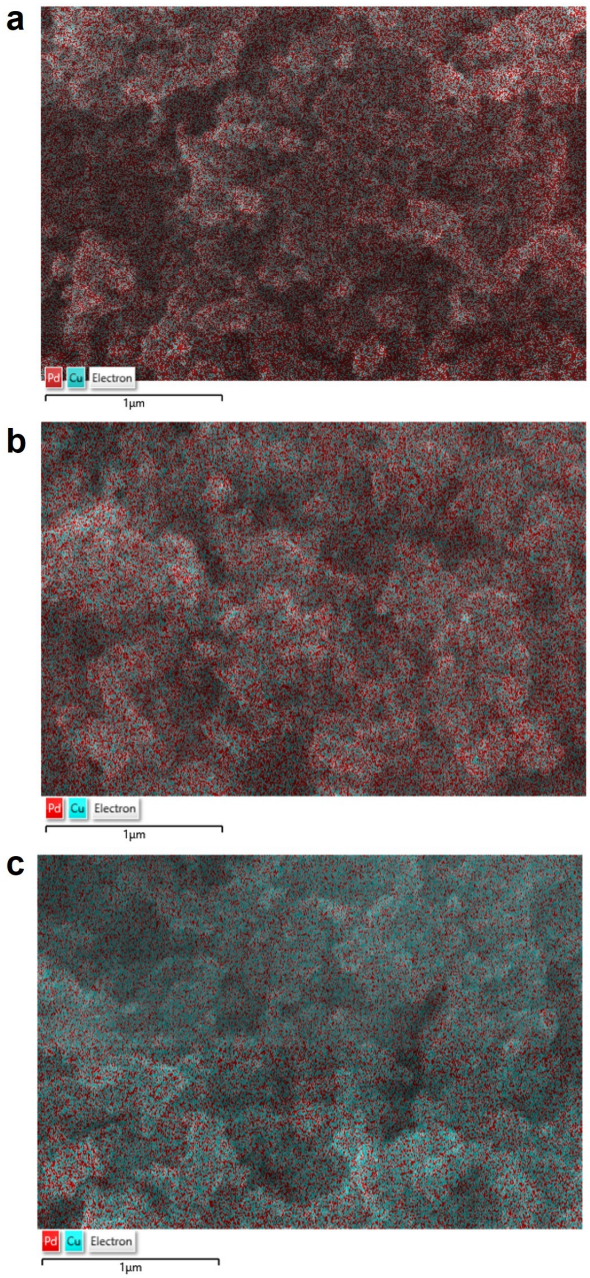

Figure S13. SEM mapping images of (a) $PdCu_{0.5}$, (b) $PdCu_1$, and (c) $PdCu_2$.

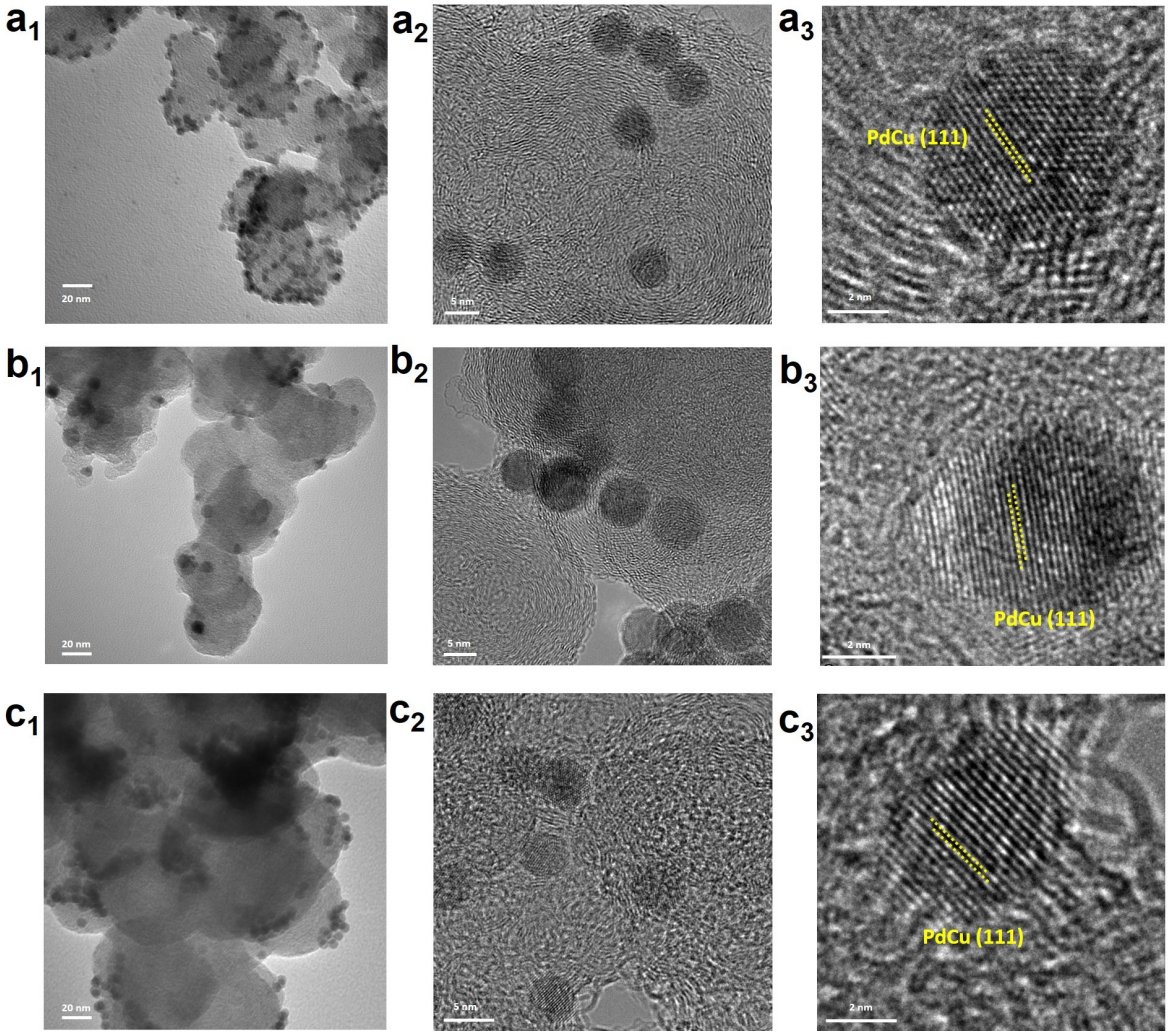

Figure S14. TEM and HR-TEM images of (a_1-a_3) $PdCu_{0.5}$, (b_1-b_3) $PdCu_1$, and (c_1-c_3) $PdCu_2$.

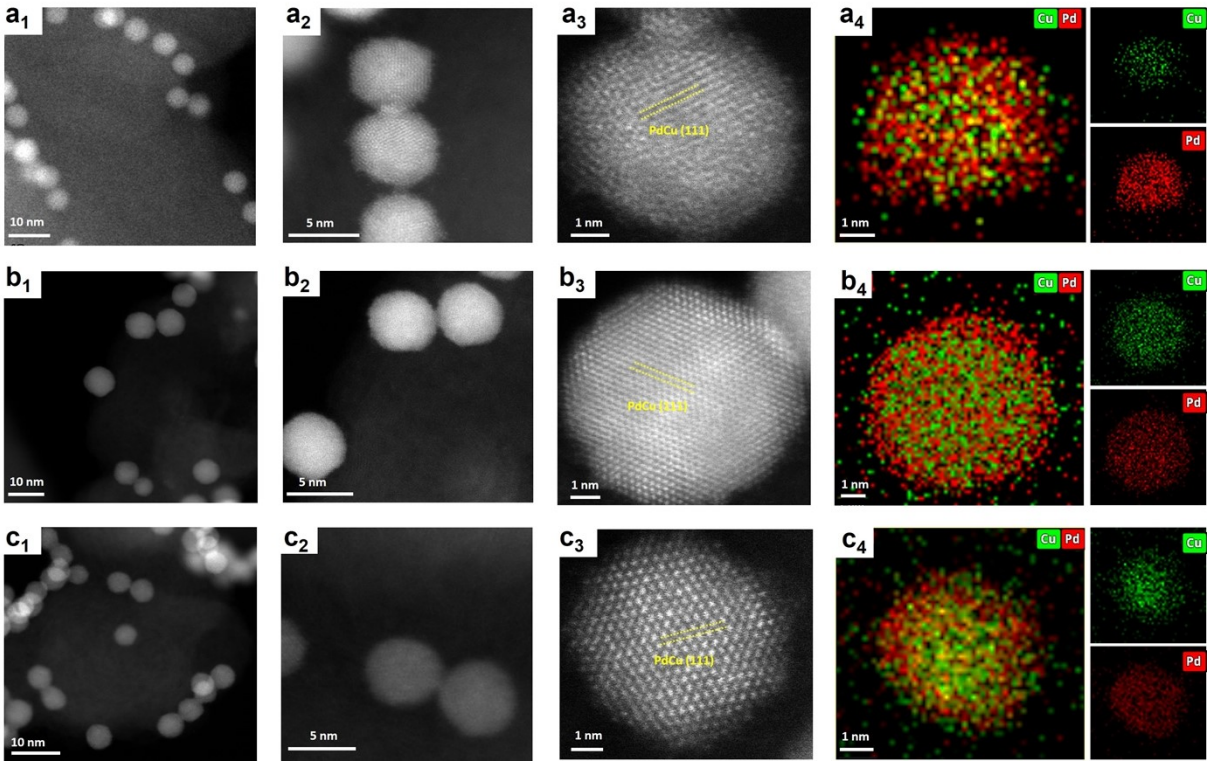

Figure S15. HAADF-STEM images with EDS element mapping of $PdCu_x$ alloy: (a_1-a_4) $PdCu_{0.5}$, (b_1-b_4) $PdCu_1$, and (c_1-c_4) $PdCu_2$.

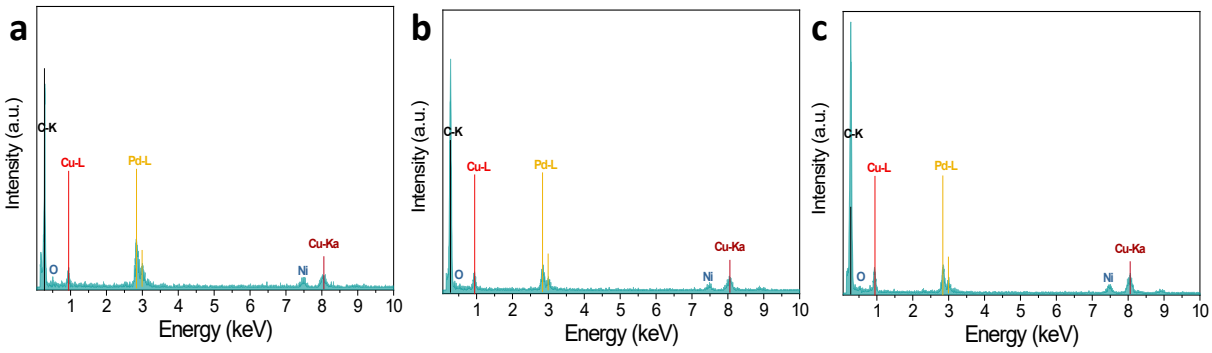

Figure S16. EDS spectra of (a) $PdCu_{0.5}$, (b) $PdCu_1$ and (c) $PdCu_2$.

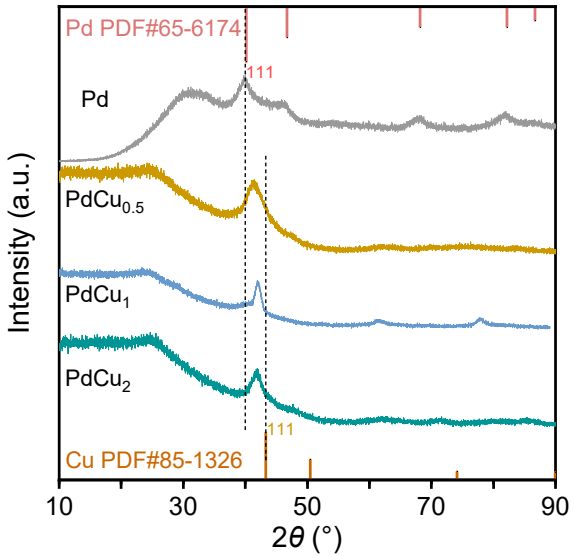

Figure S17. XRD patterns of Pd and $PdCu_x$.

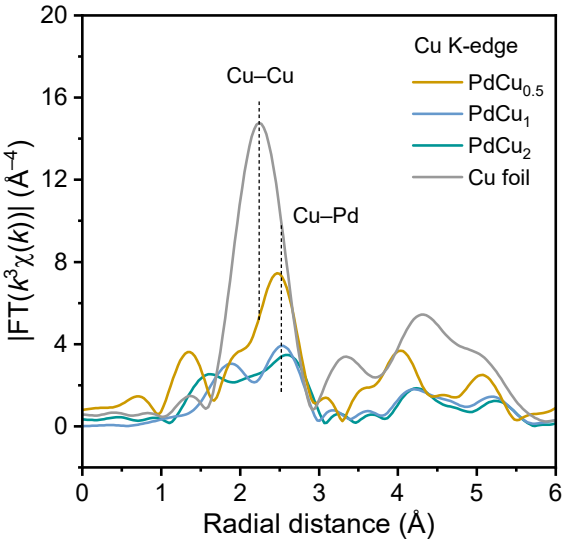

Figure S18. Cu K-edge FT-EXAFS spectra for $PdCu_x$ and reference samples.

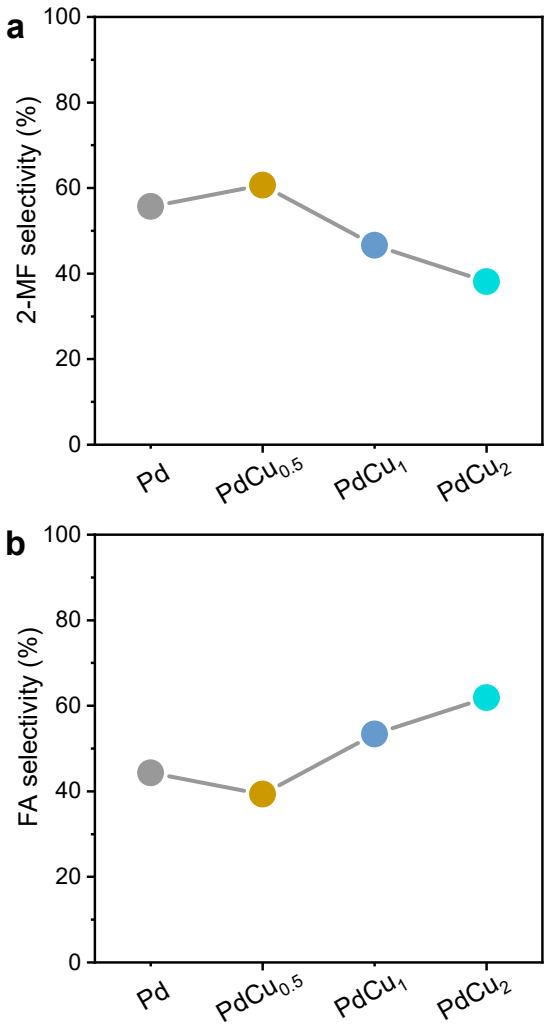

Figure S19. Selectivity of (a) 2-MF and (b) FA in Pd and $PdCu_x$ alloy catalysts.

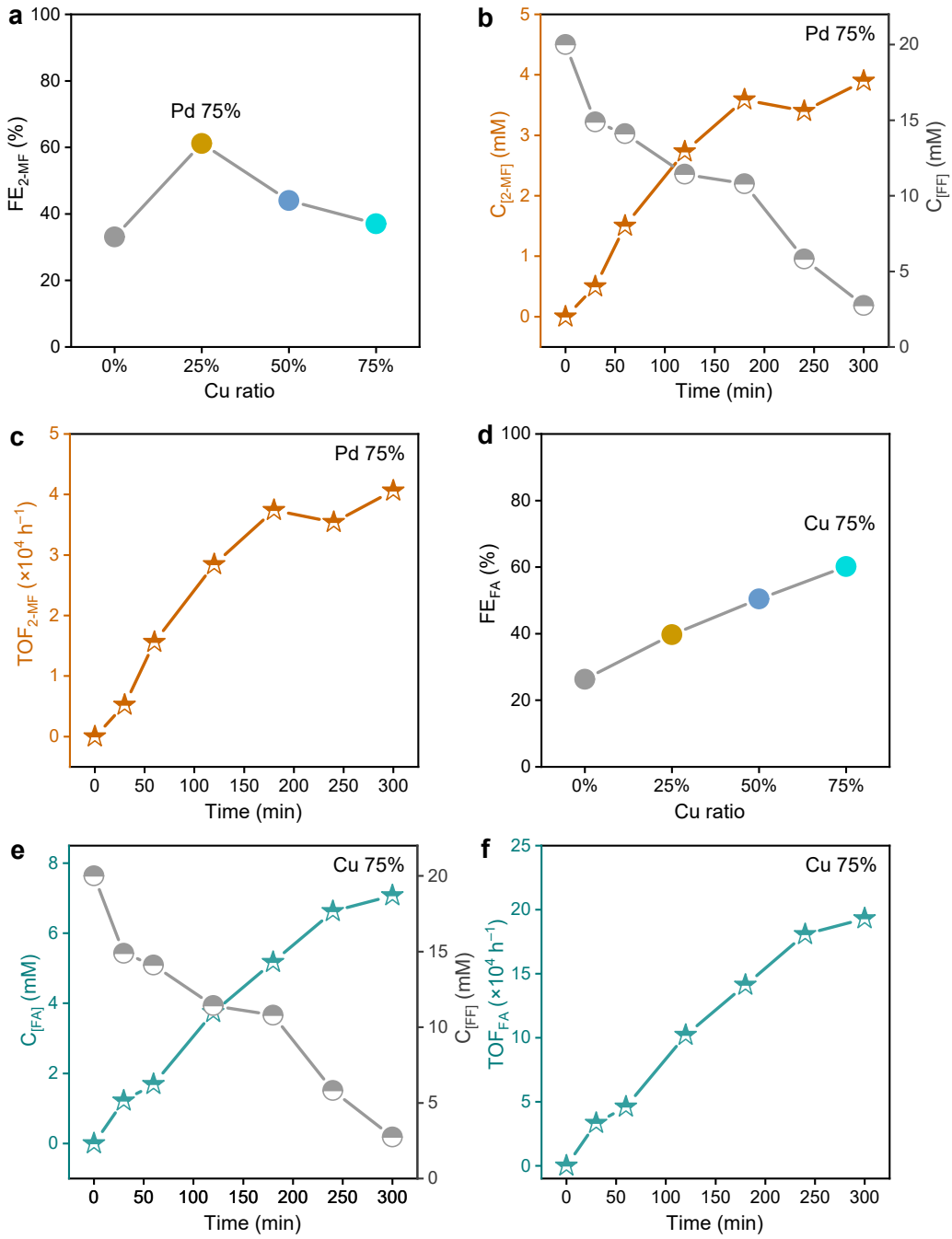

Figure S20. (a) FE of 2-MF via varying Cu and Pd ratio. (b) Concentration of produced 2-MF on Pd-rich electrode ($PdCu_{0.5}$; Pd 75%) at different reaction time. (c) TOF of 2-MF on Pd-rich electrode at different reaction time. (d) FE of FA via varying Cu concentration. (e) Concentration of produced FA on Cu-rich electrode ($PdCu_2$; 75%) at different reaction time. (f) TOF of FA on Cu-rich electrode at different reaction time.

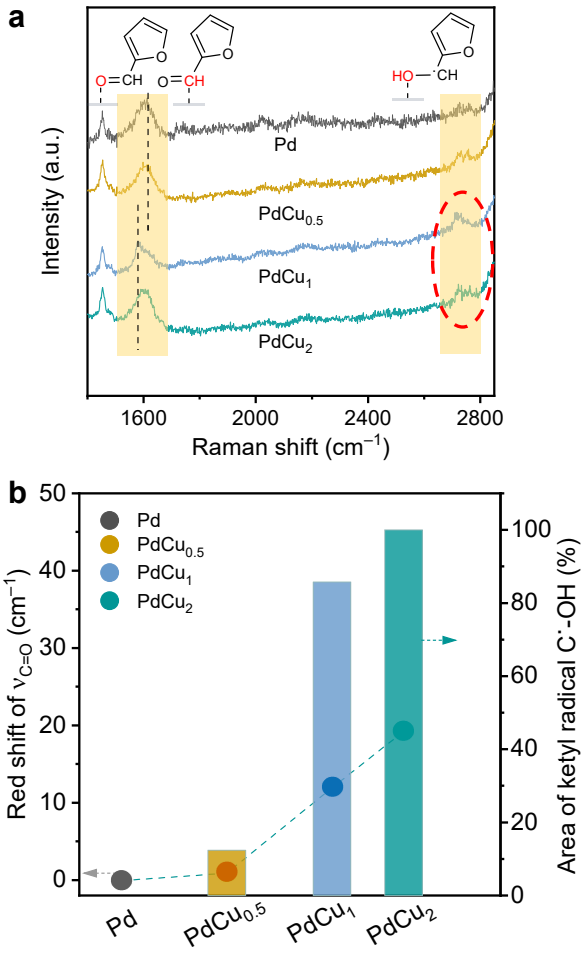

Figure S21. (a) Raman spectra of Pd and $PdCu_x$. (b) Calculated red shift of $\nu_{C=O}$ and detected ketyl radical R–C˙–OH.

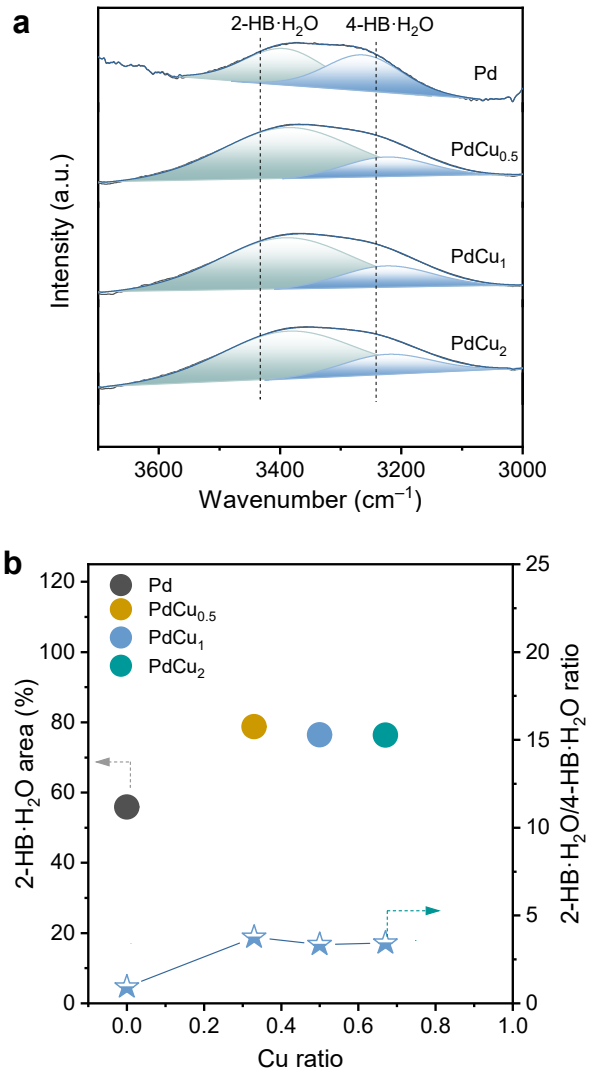

Figure S22. (a) The analysis of H_2O peak on ATR-FTIR spectra. (b) Calculated 2-HB·H_2O and 2-HB·H_2O/4-HB·H_2O ratio.

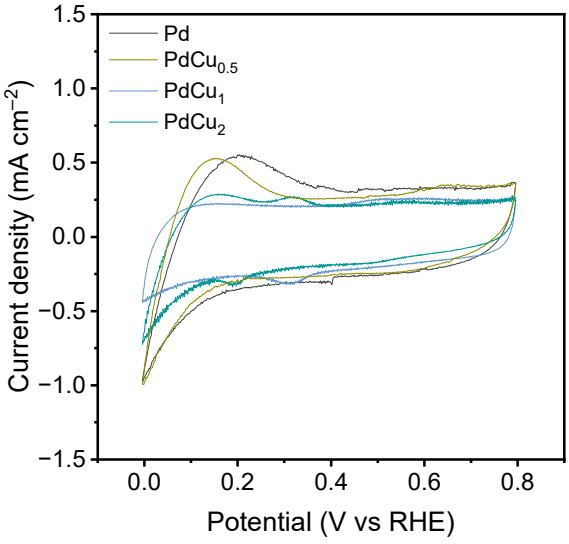

Figure S23. Typical Pb UPD CV curves for Pd and $PdCu_x$ at a scan rate of 50 mV s^{-1}.

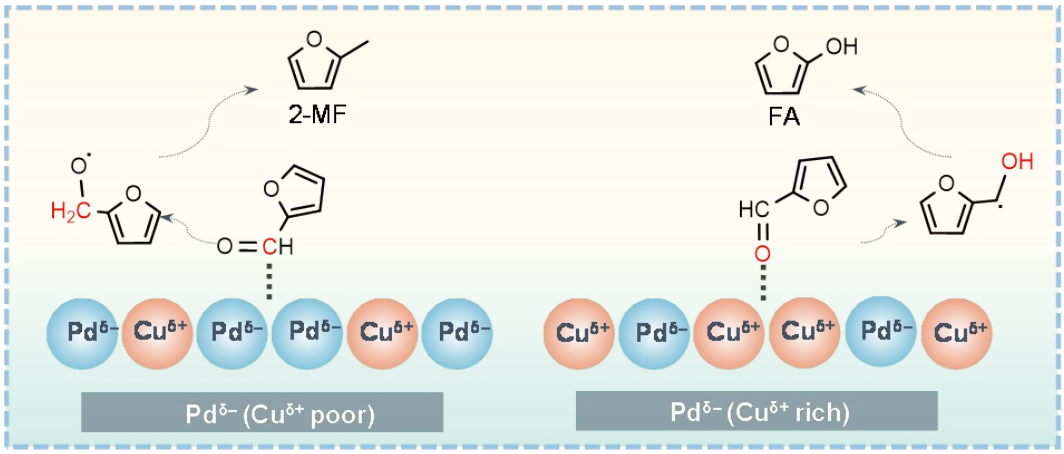

Figure S24. Schematic illustration of FF ECH selectivity control via adjusting FF adsorption configuration on tuned catalyst surfaces.

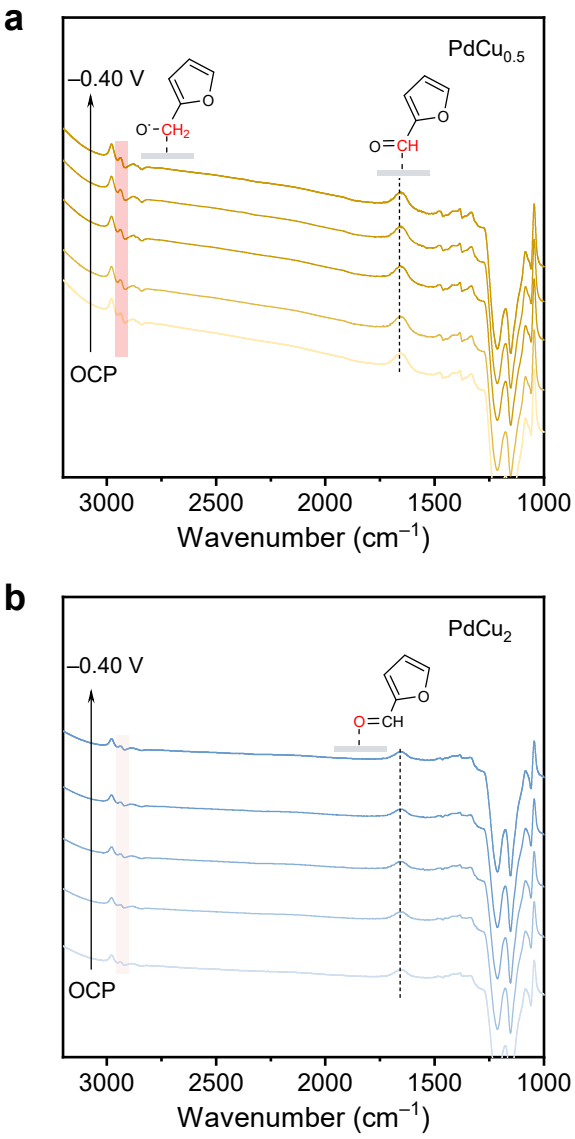

Figure S25. In situ ATR-FTIR recorded in H_2SO_4 with 20 mM furfural for (a) $PdCu_{0.5}$ and (b) $PdCu_2$.

Table S1. The Pd/Cu atomic ratio of the catalysts determined by EDX elemental mapping.

Catalyst	Pd/Cu ratio
$PdCu_{0.5}$	2.2:1
$PdCu_1$	1:1
$PdCu_2$	1:1.9